MASTER'S THESIS REPORT

Analysis of the SPERT-III E benchmark and validation of the multi-physics simulation code ANTARES

ANTOINE MARTINI

Master's Degree in Energy Engineering
Academic year 2024-2025
Matricule 219732

ANSR Tutor
Marc Forestier

School Referent Professor
Marco-Enrico Ricotti

Thanks

Thank you to IRSN, now ASNR, for welcoming me during my six-month internship.

Thanks to Politecnico di Milano, for allowing me to carry out this internship as a Master's thesis for the Energy Engineering Master's Degree.

Thanks to Marc Forestier, my internship tutor, who has supported me all along the way.

Thanks to Professor Ricotti, who was my referent Professor at Politecnico di Milano for this internship.

Thanks to Antonio Sargeni, for his unfailing support and invaluable help in solving many problems during these six months.

Thanks to the entire LSMA team for their warm welcome, and for being such a pleasure to work with.

Thank you all for having made this experience possible.

Abstract (English)

This Master's thesis took the form of a 6-month internship at ASNR, the French referent organism for nuclear safety and radiation protection. ASNR is currently developing a modern multi-physics nuclear calculation tool, ANTARES, which purpose is to better simulate incident core configurations of PWR reactors, with coupled neutronics and thermo-hydraulics computations ; and to give ASNR new and proper calculation tool for safety studies.

In this context, the internship happened at the beginning of the experimental validation process of ANTARES. In this phase, the code is tested and its results are compared to experimental ones. The SPERT III American experimental program was used as an experimental reference in this perspective. The goal of the internship was to implement a couple SPERT III test-cases into ANTARES, in order to get some first elements of comparison with the experience, and to understand the difficulties to overcome in the process of the implementation.

Four SPERT III rod ejection transient test-cases, selected for their representativity, were successfully implemented into ANTARES, and a trial and error process of parameter tuning and general setting inside the code was carried out. As a result, for each test-case, the simulated power peak was compared to the experimental one, giving rather satisfactory performance. Complementarily, a sensitivity analysis was performed, to better understand the influence of certain initial conditions and parameters on the results obtained with ANTARES.

As a preliminary experimental validation study for ANTARES, the internship gave some elements. In continuation of the experimental validation of ANTARES, after the end of the internship, the results already obtained may be refined by deeply checking the tuning of the code parameters, and more test-cases should be implemented to obtain more elements of comparison with the experience.

Abstract (Français)

Cette thèse de Master a pris la forme d'un stage de 6 mois à l'ASNR, l'organisme français de référence en matière de sûreté nucléaire et de radioprotection. L'ASNR développe actuellement un outil de calcul nucléaire multi-physique innovant, ANTARES, dont l'objectif est de mieux simuler les configurations d'accident de cœur de réacteur REP, avec des calculs couplés de neutronique et de thermo-hydraulique ; et de doter l'ASNR d'un nouvel outil de calcul approprié pour les études de sûreté.

Dans ce contexte, le stage a eu lieu au début du processus de validation expérimentale d'ANTARES. Dans cette phase, le code est testé et ses résultats sont comparés aux résultats expérimentaux. Le programme expérimental américain SPERT III a été utilisé comme référence expérimentale dans cette perspective. L'objectif du stage était d'implémenter des cas-test SPERT III dans ANTARES, afin d'obtenir de premiers éléments de comparaison avec l'expérience, et de comprendre les difficultés à surmonter au cours du processus d'implémentation.

Quatre cas-test de SPERT III de transitoires provoqués par une éjection de barres, sélectionnés pour leur représentativité, ont été implémentés dans ANTARES, et un processus d'essai-erreur de réglage des paramètres et de configuration générale à l'intérieur du code a été réalisé. En conséquence, pour chaque cas d'essai, le pic de puissance simulé a été comparé au pic expérimental, ce qui a donné des résultats relativement satisfaisants. En complément, une analyse de sensibilité a été réalisée, afin de mieux comprendre l'influence de certaines conditions initiales et de certains paramètres sur les résultats obtenus avec ANTARES.

En tant qu'étude préliminaire de validation expérimentale d'ANTARES, le stage a fourni quelques éléments. Dans le cadre de la poursuite de la validation expérimentale d'ANTARES après la fin du stage, les résultats déjà obtenus peuvent être affinés en vérifiant en profondeur le réglage des paramètres du code, et davantage de cas-test devraient être mis en œuvre pour obtenir plus d'éléments de comparaison avec l'expérience.

Abstract (Italiano)

Questa tesi di Laurea Magistrale ha preso la forma di uno stage di 6 mesi presso l'ASNR, l'organismo francese di riferimento per la sicurezza nucleare e la radioprotezione. L'ASNR sta attualmente sviluppando un strumento di calcolo nucleare multi-fisico moderno, ANTARES, il cui scopo è quello di simulare meglio le configurazioni di incidente di nocciolo di reattori PWR, con calcoli accoppiati di neutronica e termoidraulica; e di fornire all'ASNR un nuovo e adeguato strumento di calcolo per gli studi di sicurezza.

In questo contesto, lo stage è avvenuto all'inizio del processo di validazione sperimentale di ANTARES. In questa fase, il codice viene testato e i suoi risultati vengono confrontati con quelli sperimentali. Il programma sperimentale americano SPERT III è stato utilizzato come riferimento sperimentale in questa prospettiva. L'obiettivo dello stage è stato quello di implementare un paio di test-case di SPERT III in ANTARES, al fine di ottenere alcuni primi elementi di confronto con l'esperienza, e di comprendere le difficoltà da superare nel processo di implementazione.

Quattro casi-test SPERT III di transitorio di espulsione di asta di controllo, selezionati per la loro rappresentatività, sono stati implementati in ANTARES, ed è stato effettuato un processo di prova ed errore di regolazione dei parametri e di impostazione generale all'interno del codice. Di conseguenza, per ogni caso di prova, il picco di potenza simulato è stato confrontato con quello sperimentale, ottenendo prestazioni abbastanza soddisfacenti. Inoltre, è stata eseguita un'analisi di sensibilità, per comprendere meglio l'influenza di alcune condizioni e parametri iniziali sui risultati ottenuti con ANTARES.

Come studio preliminare di validazione sperimentale per ANTARES, lo stage ha fornito alcuni elementi. Nel prosieguo della validazione sperimentale di ANTARES, dopo la fine dello stage, i risultati già ottenuti potranno essere affinati verificando a fondo la messa a punto dei parametri del codice, e dovranno essere implementati altri casi-test per ottenere maggiori elementi di confronto con l'esperienza.

Summary of figures

Table of contents

Introduction : nuclear energy and its challenges

Energy is one of the core resources for our modern societies. With a reliable and clean energy available in a large amount, many of today's issues, such as achieving sustainability or protecting air quality and the environment, would be at least partially resolved. Moreover, it has been seen in recent years that energy is a strategic resource for nations to ensure their economic independence and sovereignty [1].

Among all the currently known energy sources, nuclear energy is somewhat special. In fact, to begin with, it doesn't fit well into the classic energy sources partitions. Often, fossil fuels and polluting fuels are confounded on one side, as well as renewable and green energies on the other side [2]. To understand the characteristics of nuclear energy, it is necessary to be more precise on the classic energy partitions. A fossil fuel is not necessarily polluting, even if it is usually the case, and a renewable energy source can pollute. Moreover, to be rigorous when understanding an energy source, the whole life cycle of the components have to be taken into account [3]. This means that 100% green and renewable energy does not exist, because there is always, at least, the need of materials to build and maintain facilities, which are, by essence, finite and polluting to some extent. Wind turbines could be taken as an example here [4].

The other important point here is precisely the meaning of pollution. When thinking about energies, pollution is often taken as a synonym for Carbon emission. Carbon emission is, in fact, important, but it is far from being the only possible pollution in energy production. Pollution of the air, the water, the ground, or even acoustic nuisances or spatial problems, such as the area disturbed by a dam [5]. One more important factor when speaking about energy sources, that is more and more a challenge in the modern years, is the availability of the energy. Some energies, such as those using a fuel as a heat source, are always available as long as the burner is on, some others depend on external conditions and are not controllable, such as solar or wind energies [6].

Nuclear energy, in that spectrum, can be analysed as following. It is an energy with high power production and availability. It has a very long term use potential [7]. Nuclear energy also does not directly emit any Carbon, and even taking into account the whole life cycle, including facility building and uranium enrichment, the Carbon emission to kWh produced is quite low. So, at this point, it could be said that nuclear energy is a "half renewable almost green" energy.

However, the current industry of nuclear energy faces its own big challenges, that can be summed up as so. First, a safety challenge. In fact, nuclear power uses a reaction and components that have an important risk potential, needing particularly rigorous safety measures before, during and after energy production. Second, an economic challenge [8]. Nuclear power plants and the rest of the nuclear energy chain are usually huge and need very large initial investments. And third, and not least, a political challenge [9]. Nuclear energy is complex, most people don't know how it works and many fear it based on the risks previously mentioned. Public opinion and politic decisions are a big issue for the nuclear sector, because of the duration of the projects and safety controls – usually more than a decade – that need stable guidelines and investments to be carried on properly.

Out of those three challenges, this internship focuses on the first one, the safety challenge. In the modern years, with the evolution of calculators and computers, numerical

simulation of nuclear core configurations has become more and more used, and more and more precise and reliable. Many calculation codes exist today to compute neutronics or thermo-hydraulics equations [10]. At ASNR, the new and innovative calculation code ANTARES [11] is being developed, in the aim of computing more precisely and efficiently specific configurations of the core of nuclear reactors, for the main purpose of safety studies. The goal of this thesis is to participate in the validation process of this new calculation tool.

1. Theory and context

1.1. Nuclear safety in France, ASNR

As previously mentioned, safety is one of the most important challenges of nuclear energy production. It is a very wide topic, because it means avoiding incidents along the entire industrial cycle, and being able to limit the effects if one was to happen [12]. To be exact, the French law says *« Nuclear safety is the set of technical and organizational measures relating to the design, construction, operation, shutdown and decommissioning of basic nuclear installations, as well as to the transport of radioactive substances, taken with a view to preventing accidents or limiting their effects »* [13].

Nuclear safety matters includes, for example, the physical disposition of the reactor, with several containment barriers ; several redundant automations and systems to control the operation of the reactor ; or even the very typology of reactor used [12]. Nuclear safety also seeks to predict every possible incident and control what happens in the eventuality of one happening, from the mitigation of the incident itself to the protection of people and environment [12].

In France, the main actor of nuclear safety control is the ASNR, the French Nuclear Safety and Radiation Protection Authority, that results from the recent fusion between the ASN and the IRSN [14]. Historically, the ASN, the Nuclear Safety Authority, is the administrative authority regulating nuclear safety [15] ; and the IRSN, Nuclear Safety and Radiation Protection Institute, is the expertise reference for nuclear safety and radiation protection [16].

1.2. Nuclear generalities

In this paragraph, some general nuclear tools and knowledge useful for the following of this document, will be introduced, without going into too many details.

First, a very quick overview of the working principle of a nuclear reactor can be presented. Industrial nuclear reactors use the fission reaction. Large nuclei are packed together into the reactor core, and a controlled chain reaction is provoked. Some large nuclei are broken into smaller nuclei, releasing some neutrons and a huge amount of energy. The neutrons are like small projectiles that will hit other large nuclei, breaking them in their turn, continuing the chain reaction [17]. In nuclear reactors, the chain reaction is well-controlled, producing a stable amount of power. This results in a very large amount of heat, that is then transferred to a coolant fluid system to evacuate and use the energy.

Neutrons play a key role in the equilibrium of a nuclear reactor. Their amount and where they go is determining. A very useful concept to describe neutron behaviour is cross-sections [18], [19]. A cross-section represents a probability of reaction. To each nucleus inside of the core are assigned characteristic cross-sections ; a capture cross-section, a fission cross-section and a scattering cross-section. For example, an element with a large capture cross-section will have a high probability of absorbing an incoming neutron. Cross-sections are measured in barns, homogeneous to a surface.

During the nuclear chain reaction, a lot of new nuclei are formed, because fission of the large initial nuclei does not always produce the same fragments [20]. Each one of those nuclei has specific cross sections, that can change the nuclear equilibrium over time. Another important point about cross-sections, is that they are not constant, they depend on the energy of the neutron. A high energy neutron and a low energy neutron will not encounter the same reaction cross-sections [21], [19].

Various typologies of nuclear fission reactors exist [22], because several different large nuclei can be used as a fuel (Uranium or Thorium for example), and also various strategies exist to handle the neutrons. Neutrons emitted by a fission reaction have a rather high energy, that they will gradually lose over time. Some reactors mainly use “fast neutrons” (high-energy), while others use “thermic neutrons” (low-energy) [23]. The goal being to avoid as much as possible neutron absorption by other elements.

The major part of the French nuclear industry uses PWR (Pressurized-Water-Reactors) fission reactors [24]. This typology of reactors uses mainly enriched Uranium as a fuel, and high-pressure water as a coolant. Low-energy neutrons are used in this type of reactor, contrary to SFR (Sodium-cooled Fast Reactors) for example [25].

To simplify a lot, k_effective, or k_eff, is the variable that represents the neutron equilibrium inside the nuclear core [26]. It is, practically, the amount of neutrons released on average by the fissions occurring in the core at the generation N+1, divided by the same quantity at the generation N. A k_eff equal to 1 corresponds to an equilibrium, called criticality of the nuclear core. A reactor core with k_eff greater than 1 is overcritical, and subcritical if k_eff is smaller than 1.

Among the neutrons inside the core during the chain reaction, the major part, called prompt neutrons [27], is directly coming from the fission reactions. A small amount, called delayed neutrons, comes from the radioactive decay of other nuclear elements, which takes some time, going from milliseconds to minutes depending on the elements [28], [29]. Delayed neutrons are important because their existence helps a lot maintaining the equilibrium of the chain reaction. Their proportion in the total amount of neutrons is called Beta_effective, or Beta_eff, and is in the order of magnitude of a percent, or a bit less [30].

Delayed neutrons are also used to define the reactivity in $, that will be useful in this document. The reactivity is defined as the ratio of k_eff-1 over k_eff, and the reactivity in $ is the reactivity divided by Beta_eff, so that 1 unit $ of reactivity corresponds to the reactivity of the delayed neutrons [31].

1.3. Nuclear computations and ANTARES

Nuclear computations have always been important, to predict and understand as precisely as possible the behaviour of the reactor and limit the necessity of physical testing. With the increasing power of computers, many nuclear calculation tools have been created [10]. Generally, there are calculation codes performing neutronics calculations, solving neutronics equations to simulate the state and behaviour of the nuclear core depending on its configuration

; and there are codes than tackle the thermo-hydraulics physics. Those codes model and simulate the behaviour of the core and its surroundings, focussed on heat transfers and matter flows. More rarely, because it is a big challenge, there are codes that handle both, called multi-physics codes [32].

In all the cases, nuclear calculation codes are very complex, meaning that the creation and validation of a new calculation tool takes time, the calculations can be quite long, and some reactor configurations are too complex to be tackled and need simplification. This high complexity is also why usually the calculation codes focus on either the neutronics side or the thermo-hydraulics side. A neutronics calculation tool usually has a small thermo-hydraulics module integrated to enable calculations – and vice-versa – but not a full thermo-hydraulics calculation tool.

Before going further, a few more specifications can be enlightened about nuclear calculation codes. Most codes are deterministic, discretizing physical equations to solve them, but some Monte-Carlo neutronics codes do exist, simulating numerous virtual lives of a neutron into the core and then observing the results, instead of directly solving equations.

Also, usually nuclear calculation codes are designed to tackle only one specific type of reactor, for example PWR [24], or SFR [25]. PWR are Pressurized Water Reactors, working with enriched uranium and using slow neutrons, and are studied a lot because they represent the wide majority of industrial reactors used to produce energy, at least in France. SFR, Sodium-Cooled Fast Reactors, are a very different type of reactor, studied mainly for research, and different calculation tools are used for them.

Moreover, neutronics calculation codes in particular can be specifically designed to compute degraded configurations of the nuclear core. In general, degraded configurations are harder to simulate than normal operation, but they are particularly interesting when it comes to nuclear safety, because degraded situations happen during incidents, and it is particularly important to understand and control those cases.

ANTARES is a new calculation tool developed at ASNR. Its double ambition is to better connect neutronics and thermo-hydraulics computations, and to provide ANSR with its own modern calculation tool for nuclear safety studies. More specifically, ANTARES is designed to perform coupled deterministic neutronics and thermo-hydraulics computations on incident configurations for PWR reactors.

ANTARES [11] is the coupling of PARCS [33] (resolving 3D core neutronics with nodal methods and a multi-parameter cross-sections library generated by CASMO5 [34]) and CATHARE-3 [35] (core and system thermal-hydraulics). These two codes are coupled via an exchange of 3D fields (power from PARCS to CATHARE and fuel temperature, density and temperature moderator, boron from CATHARE to PARCS) and the exchange is driven by some internal routines (in Fortran) of ANTARES. In a steady state computation, there is an exchange every time step until the user-defined convergence criteria are reached ; for a transient, the coupling is explicit : in each exchange the time is incremented.

The structure of ANTARES is shown in the following picture:

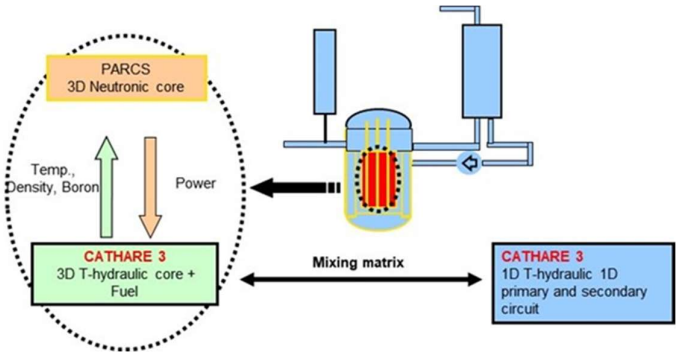

Figure 2. ANTARES structure [11].

For SPERT computations, PARCS works with two energy groups (thermal, energy less than 0.626 eV ; fast : energy bigger than 0.625 eV) ; radially, one node by assembly (due to the small assembly pitch, 7.62 cm, it is not necessary to use more than one node by direction) ; axially with a quite big number of meshes – which will be further discussed in the part 2.3.D. – to better catch the flux gradient. A channel by assembly was defined for the thermal-hydraulic core as well.

1.4. The SPERT-III E core

The Special Power Excursion Reactor Tests project was established in the US in 1954, as part of a US reactor safety program, to experiment with the kinetic behaviour and safety of nuclear reactors [36]. In particular, in 1958, the SPERT-III reactor facility was built to conduct reactor behaviour and safety studies under operating conditions typical of pressurized-water and boiling-water reactors. The main objective in the SPERT-III facility design was to perform power excursion tests and gather information on the kinetic behaviour, on a reactor designed similarly to pressurized water power reactors (industrial PWRs) in order to investigate on safety problems common to this class of reactors.

The SPERT-III E core [37] (also simply called SPERT-III) can be assimilated to a very small research-purposed PWR core. It is composed of 64 assemblies, each measuring approximately 8 cm by 100 cm, for a core that has a height of a meter and a diameter of a bit less than a meter. In comparison, industrial PWRs are typically 4 meters tall and 3 meters wide, containing 144 to 204 assemblies [38]. The structure of the core, apart from the size, is very similar to the one of PWRs, making SPERT III a very good experimental facility to better understand the behaviour of PWRs.

SPERT III, being made for power excursion tests, was mainly designed to operate fast transients with low total energy release, and not sustained reactor power episodes, contrary to industrial PWRs. Also, the nominal power of the SPERT III E core is 20 MW, whereas usual industrial reactors are closer to the GW.

Inside the core are two neutron-absorbing rod clusters, the control rod cluster, distributed radially in the core, to control the equilibrium of the reaction, and the transient rod cluster in the centre, designed to be ejected during the experimentations.

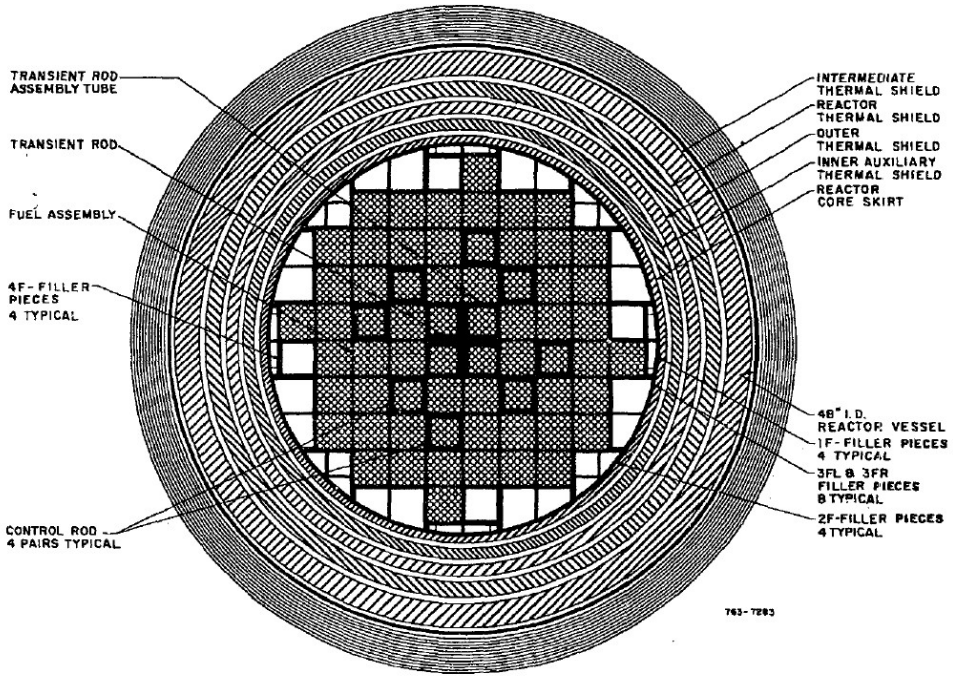

Figure 2. SPERT-III E core cross-section [37]

Despite its small size and old age, the SPERT III core and its experimental program are quite precious for various nuclear studies. In fact, physical testing of nuclear incident configurations is, understandably, quite rare, and the tests carried on with SPERT III are virtually the only tests of this kind that have been run on a PWR core.

Moreover, a large amount of various tests was run during the SPERT III program [38]. The tests conducted mainly consist of an ejection of the transient rod, causing a core reactivity insertion. Many different tests were performed, varying initial parameters such as the initial core power and temperature. Then the response of the core to the reactivity insertion can be observed, with, in particular, the duration and strength of the power peak after the experimental incident.

1.5. The validation process

As previously mentioned, nuclear calculation tools are usually very complex codes. It takes a long time to develop them, and when they are developed it takes a long time to test them. Every software follows a testing phase at the end of its development. For the case of nuclear calculation codes, this phase, the “validation” phase, is very special.

The validation process is a long and complex process that is, in France, strictly ruled by the ASN, Nuclear Safety Authority, with the [39]. It follows several specific steps. The deep verification of the code comes first, then the validation of the models used in the code, and finally

the integral validation and comparison of the results obtained by the code to other results, either obtained by other already validated calculation tools, or even better experimental results.

Another interesting point that can be mentioned here, is that the validation process of a nuclear calculation tool does not concludes on a yes/no answer, such as “yes the code works”, or “no it doesn’t”. It is more complex than that, because simulations are approximate and the behaviour of the code is complex, and a lot dependant on configurations simulated, and initial conditions. The same calculation tool, for example, could work pretty well on large PWR cores at steady state and low power, and work pretty poorly on other configurations and conditions. So the process of validation of a calculation tool rather gives a certain level of confidence to the code, in the tested configurations. After that validation phase, the more the calculation tool is used, the more confidence it can get, depending on the results gotten and the configurations and conditions tested.

1.6. Context of the internship

This internship was hosted from September 2024 to March 2025 by the French Institute of Nuclear Safety and Radiation protection (IRSN) the French nuclear safety expert, that merged in January 2025 with the ASN (Nuclear Safety Authority), becoming the ASNR. More precisely, the hosting structure was originally IRSN/PSN-RES/SEMIA/LSMA [40].

The goal of the internship was to contribute to the validation process of the new calculation tool ANTARES, with comparisons to SPERT III experimental results. The first version of the code have been fully developed, and a second version is in current development [11]. The validation study is performed using ANTARES version one. The most code-deep and model-specific steps of validation have already been done, and this internship is situated at the very beginning of the last validation phase, the generation of results with the code and their confrontation to other results, in particular experimental ones.

For this internship, it was decided to use SPERT III experimental results as a reference to compare with when generating results with the calculation tool ANTARES. The goal is to implement into ANTARES the SPERT III core data and to tune all the parameters and conditions correctly to be able to simulate various SPERT III experiments with ANTARES.

Among the large amount of experiments conducted in the SPERT III program [38], 4 reference test-cases were chosen for the internship, that will be further detailed in the next part. These 4 specific reference test-cases were chosen because they are quite representative of the variability of initial conditions for the experiments, such as initial power and temperature. What is more, those test-cases are often among the studied ones in the existing literature, making them particularly interesting to implement, because several result comparisons will be possible.

The internship happened at the very beginning of testing real test-cases with ANTARES and the final validation step. It was useful in the context of ANTARES development as a sort of preliminary experimental validation study, aiming to setup all the data and parameters correctly into the code and make some first test-cases run with ANTARES, to get some first results to study and to solve potential issues encountered when implementing the data and running the code. For

a complete validation process of the code with the experimental comparison, the files and data will have to be checked more in-depth, and more SPERT III test-cases will be simulated with ANTARES to get more elements of comparison.

2. Work carried out with ANTARES and presentation of the results

2.1. Implementation of the test-cases into ANTARES

Among the large amount of experiments conducted in the SPERT III program [38], 4 reference test-cases were chosen for the internship, the test-cases t60, t70, t81, t86. These 4 specific reference test-cases were chosen because they are quite representative of the variability of initial conditions for the experiments, such as initial power and temperature.

A good summary of the documentation and experimental data about SPERT III can be found in [38]. The key inputs for the experimental rod ejections are the resulted reactivity insertion, and the initial core temperature and power. The key information is listed in the Figure 3, as well as the main experimental results, the height and time of the power peak following the rod ejection.

	t60	t70	t81	t86
reactivity insertion ($)	**1.23** +/- 0.05	**1.21** +/- 0.05	**1.17** +/- 0.04	**1.17** +/- 0.04
temperature (°C)	**260** +/- 2	**120** +/- 2	**260** +/- 2	**260** +/- 2
power (MW)	**5,0E-05**	**5,0E-05**	**0.9** +/- 0.1	**19** +/- 1
power peak (MW)	**410** +/- 41	**280** +/- 42	**330** +/- 30	**601** +/- 60
power time (ms)	**227** +/- 5	**200** +/- 1	**135** +/- 3	**110** +/- 5

Figure 3. Main initial conditions and experimental results for the four selected SPERT test-cases

The datasets of the SPERT III core were already existing for PARCS, and with a few adaptations, it was possible to use them with ANTARES as well.

The test-case t60 was the first one to be implemented, and a lot of issues were solved thanks to this process, so the test-case t60 will be taken as an example for the implementation. There are some minor differences when implementing the others test-cases but the process is very similar.

2.2. The SPERT III experimental data

The SPERT III experimental tests, as mentioned earlier, are quite old. The existing data has been gathered in [38]. In the experimental documentation, some data is approximate, and some is missing. It is possible to work with the data available, but the missing information causes some complications and imprecisions. The encountered issues were the following.

About the coolant flow rate into the core, the only data available was the speed of the fluid, given in fps (feet per second). For the computations, the mass flow rate is needed. It was

necessary to compute the flow section of the coolant and its density at the given temperature to access the mass flow rate, which is detailed in the next part.

Probably the most difficult missing point, the experimental documentation does not mention the initial positions of the two control rods groups. The only available data to work with is the reactivity insertion. The detailed process for resolving this issue can be found in [this paragraph].

Also, the only information about the rod ejection trajectory is a constant ejection acceleration for the transient rods, that is always the same, for all the different testing configurations. There is no uncertainty given on this data, and it could be a source of imprecisions.

2.3. Implementation of the test-case t60

In this part, the whole implementation process will be described, taking as an example the test-case t60. The main steps of the implementation will be explained, and then the results obtained will be presented, discussed and compared to other references. For all this part, only the test-case t60 is presented, the test-cases t70, t81 and t86 will be tackled separately in the part 2.4.

2.3.A. Evaluation of the mass flow rate

About the flow rate, the main information available in the experimental documentation is the velocity of the coolant, 14 fps, which is approximately equal to 4.267 m/s. Other key known data are the technical specifications of the core, and the temperature of the coolant.

First, the density of the coolant can be evaluated. The coolant is simple water inside the core, at a pressure of 103.4 bar and a temperature of 260°C (for the t60 case). With Octopus, a small tool used at LSMA, a density of 790.63 kg/m3 was found in these conditions.

Then, the flow section has to be evaluated. First, the total assembly section has to be accounted. There are 52 assemblies with 25 fuel rods, each with a 2.975 inch side square section, which is a 57.15 cm2 section per assembly. There are 4 assemblies with 16 rods, each with a 2.476 inch side square section, and 8 control rods with the same section, which is a 39.56 cm2 section per assembly. The total assembly section adds up to 3446 cm2. Then, with all those assemblies, there is a total of 1492 fuel rods, each with a 0.466 inch circular section, which is a 1.09 section per rod. The total rod section adds up to 1630 cm2. Assuming that the fluid only flows into the assemblies, the flow section can then be evaluated at 1816 cm2 or 0.1816 m2.

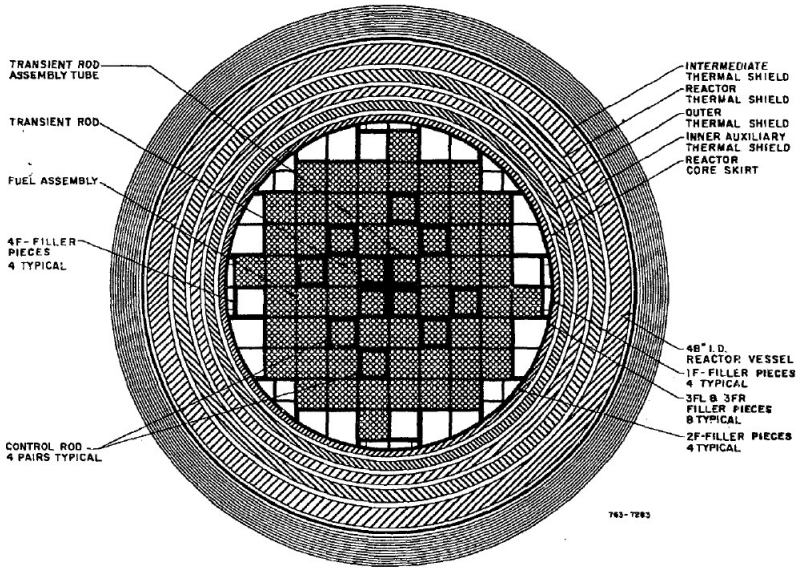

Figure 4. SPERT-III E core cross-section [37]

Finally, the mass flow rate can be found as the velocity of the flow, multiplied by the density of the fluid and the section of the flow. As a result, a mass flow rate of 10.32 kg/s in found.

There could be some imprecisions in the mass flow rate evaluation, such as imperfect flow section estimation, but a possible minor imprecision on the value of the mass flow rate is fine, as a small difference in the mass flow rate of the coolant should not impact much the behaviour of the core on a very small time period. Experimental tests last less than a second, making thermic effects in the coolant quite small.

2.3.B. Evaluation of the initial positions of the control rods

There are two distinct groups of control rods inside the SPERT III E core. The first rod group is radially distributed into the core, consisting of 8 identic rods : this first group is called the control rod cluster (BCT). The second rod group is made of the 4 central rods, that is called the transient rod cluster (BTR). In fact, the experimental test-cases consist of the ejection of the transient rod cluster, causing the power peak to happen. Particular attention will be given to these two rod clusters in this part. In the rest of the report, the term control rod may be used to refer to all the rods, by abuse of language. Rod clusters might simply be called “rods” as well.

So, for all the rod-ejection experimental tests, in the initial state both the rod clusters are inserted into the core ; and in the ending state, after the transient rod ejection, the control rod cluster has not moved and the transient rod cluster is fully out of the core. The position of the rods is measured in extracted steps from 0 to 101 (1 step = 1.026 cm), meaning that the position 0 corresponds to a fully inserted rod, and the position 101 corresponds to a fully extracted rod. The initial position of the two rod clusters will be named, respectively, z_ct for the control rod cluster, and z_tr for the transient rod cluster. A basic representation of the rods positions before and after the ejection is represented on the Figure 5.

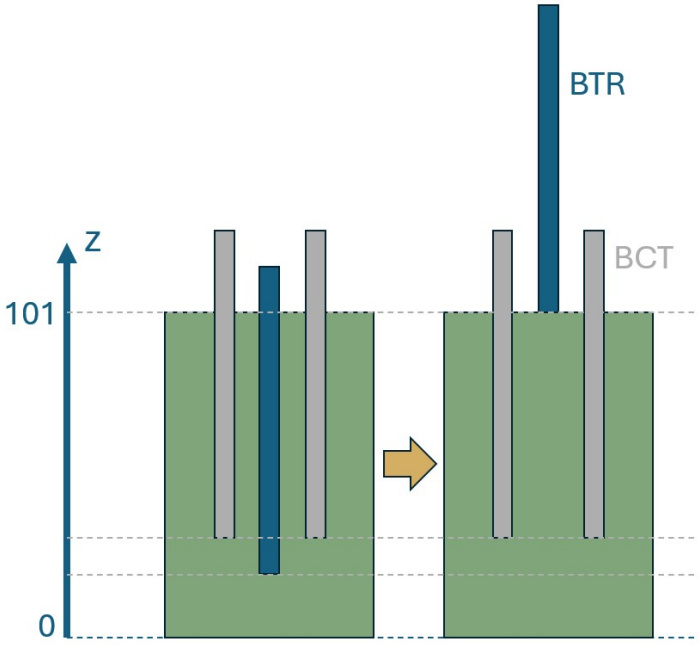

Figure 5. Rudimentary diagram of the rod positions before and after the ejection

Aside from this, the known data about the ejection of the transient rod cluster ejection are the reactivity insertion between the initial state and the end state, and the fact that in the initial state core criticality is respected. Plus, the configuration of the core and the initial conditions of the test, such as temperature and power are known.

The method used here to deduce the initial position of the two rod clusters was already successfully used in other studies such as [41] and [42]. It is possible to deduce, first, the position of the control rod cluster, and then the position of the transient rod cluster, using an empirical approach by simulating static configurations with ANTARES to guess the missing data thanks to an empirical process close to dichotomy.

In a first step, the final configuration is studied : the position of the transient rod cluster is known, as well as the reactivity of the core and the rest of the core data. From these data and with the fixed z_tr, it is possible to simulate the static configuration of the core with a hypothetic z_ct into ANTARES, and check how close the core reactivity is to the desired one, which is 1.23$ here for the test-case t60. With more and more precise tuning of z_ct, it is possible to find precisely the value of z_ct that causes the core to have this reactivity in these conditions.

In a second step, the initial configuration is studied. Now the position of the control rod cluster is known, and also the fact that the core is critical at this state. So, similarly to step 1, an empirical simulation process is performed with ANTARES, with static configuration simulation, where z_ct is now fixed, and the value for z_tr is adjusted along the process to get closer and closer to criticality.

This empiric simulation process can be a bit long, because ANTARES calculations take a bit of time, but as the simulations performed here are static, the computations are still quite fast,

and satisfying results can be achieved in a reasonable amount of time. For the test-case t60, z_ct = 43.129 and z_tr = 32.877 were found with this process, in extracted steps units.

2.3.C. Ejection trajectory

For ANTARES to work, it is necessary to manually insert the position of the transient rod, time step by time step. Knowing the constant acceleration of the rod during the ejection – 50.8 m/s^2 according to experimental data [38] – and the starting position, thanks to the previous empirical simulation study, it is possible to get the step-by-step position of the rod, plotted on the Figure 6. A time step of 5 ms was used for the ejection trajectory. The ejection lasts about 170ms. For this step of the implementation, it can also be kept in mind that there is no uncertainty associated with the value of the acceleration in the experimental documentation, which will be discussed later in this report.

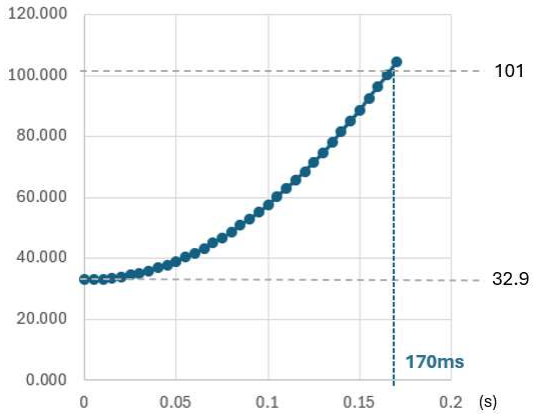

Figure 6. Discretization of the rod ejection trajectory (extracted steps units)

2.3.D. Mesh testing

With all the data implemented, missing parts completed and parameters tuned, at that point, it was possible to start simulating the test-case t60 with ANTARES. One of the last important factors for the simulation is the spatial mesh used for the calculations. In fact, ANTARES uses PARCS and CATHARE, two deterministic codes, that work by discretizing equations to be able to solve them. The discretization spatial step can be tuned, and it is a key factor, because, generally, a too large spatial step means imprecisions in the results, and a too small spatial step means a very time-consuming computation.

Radially, the default mesh setup will be used, which consists of 4 mesh per assembly for PARCS and 1 mesh per assembly for CATHARE, as explained in the part 1.3. There is a lot more potential variability on the number of axial meshes, which is the next point.

To tune the axial spatial step of the simulation mesh, it is possible to manually set the number of axial meshes into PARCS and CATHARE. Some testing has been done to get an idea of a good mesh size.

First, for PARCS, some static tests with both rod clusters inserted were performed and the variability of the value of k_eff was taken as an indicator of the convergence of the calculation. PARCS seems to converge reasonably with 70 or more axial meshes, and it was observed that it is not possible to go over 100 meshes with PARCS, the computation can be done yet with this amount of meshes. As a good compromise, it was decided to set further computations on 80 axial meshes for PARCS. Static tests are quite fast, which was convenient.

PARCS mesh	K_EFF
10	0,977622
20	0,98138
40	0,981906
50	0,98252
60	0,982223
70	0,982397
80	0,982445
90	0,982415
95	0,982454
100	crashes

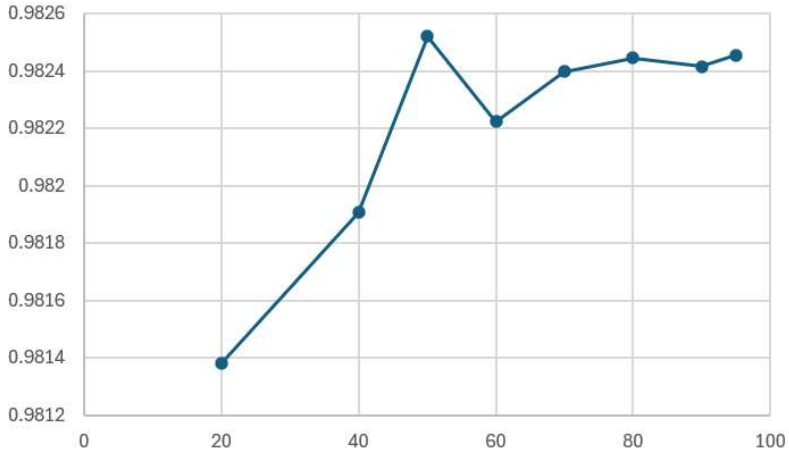

Figure 7. PARCS convergence depending on the number of axial meshes

Then, for CATHARE, it was chosen to simulate the complete transient, with the initial rod positions found earlier, and to take the variability of the time and height of the power peak as an indicator of the convergence. Transient tests with CATHARE can be quite long, and the duration depends a lot on the amount of axial meshes chosen, from one to ten hours roughly. For the t60 test-case, very little variability was observed in the results when modifying the amount of axial meshes. The short time period of the transient, less than a second, and the low initial power for the t60 test-case, might cause thermic effects to be small during the transient, and make this variability small here. This might be different for other test-cases. For now, an amount of 30 axial meshes for CATHARE was chosen, as it seemed to be a good compromise between good convergence and computation duration. The computations took about a couple of hours with this setting.

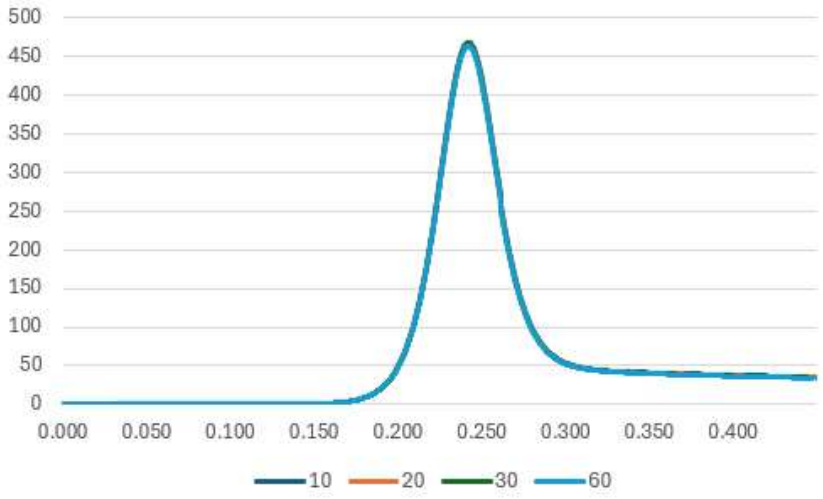

Cathare mesh	power peak time	value
	ms	MW
10	242	468,6
20	242	466
30	242	465,4
60	242	463

Figure 8. CATHARE results depending on the number of axial meshes

2.3.E. Results

With all the setup previously explained, it was possible to start making full simulations with ANTARES and obtain some first results for the t60 test-case. As can be seen on the graph, the ANTARES-simulated power peak is not that far from experimental results. According to the experimental data, the t60 test-case has a power peak of 410 MW, 227 ms after the beginning of the rod ejection. On the simulation side, ANTARES results show a power peak of 465 MW at 242 ms. Thus, there is a delay of 15 ms and a deviation of 55 MW in the height of the peak, that is a 13.4% deviation.

	t60
reactivity insertion ($)	**1.23** +/- 0.05
temperature (°C)	**260** +/- 2
power (MW)	**5,0E-05**
power peak (MW)	**410** +/- 41
power time (ms)	**227** +/- 5

Figure 9. Main initial conditions and experimental results for the test-case t60

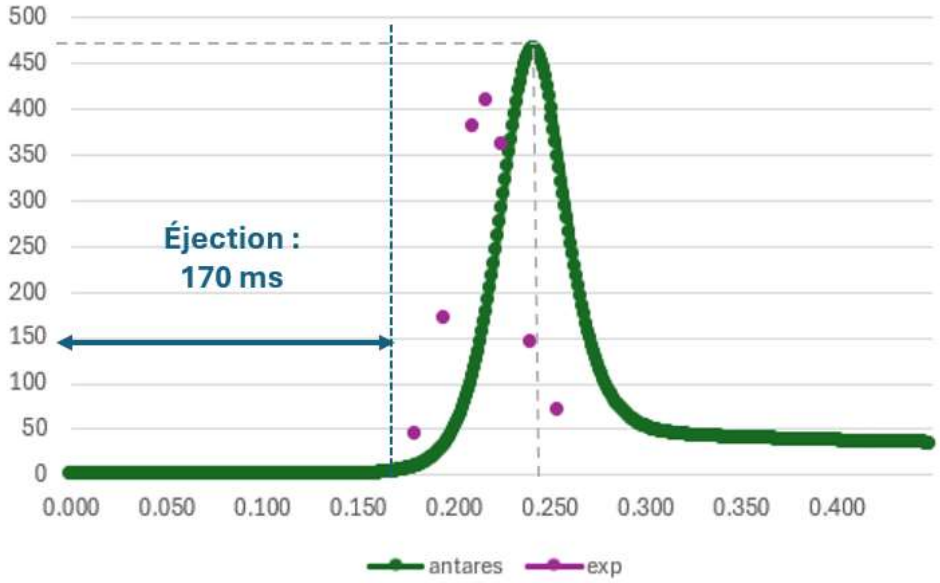

Figure 10. First t60 ANTARES results compared with the experimental power peak

At this point in the study, the computations were not done with the best parameter settings for precision of the results. As lots of simulations had to be done in order to adjust everything, it was necessary to perform lots of them, and it was better to have slightly less precise results but much faster computations. The most important example of this is the time-step of the computation. This time-step determines how large the time-discretization is in the simulation, and a key factor in the fast computation-precise computation equilibrium. For the previous results, a 1 ms time-step was used. Then, some more simulations of the same test-case t60 were performed with a smaller time-step, up to a tenth of the original one. The computations took more time, up to 7-8 hours, but there was an interesting variation in the results.

When reducing the computation time-step, the time of the power peak does not change. However, there is a slight change in the power peak value, in the direction of the experimental results. Experimentally, the test-case t60 has a 410 MW power peak. With the reduction of the time-step, the value of the power peak goes from 465.4 to 450.8 MW, making the deviation go from 13.4% to only 10%. This is not huge, but still significant. It can also be noted that this slight improvement in the results allows ANTARES to get into the experimental uncertainty margin, the experimental uncertainty on the power peak value being 410 +/- 41 MW.

calculation time step	peak time	peak power
ms	ms	MW
1	242	465,4
0,5	242,5	456,2
0,25	242,5	452,6
0,1	242,7	450,8

Figure 11. Evolution of ANTARES results with the decrease of the calculation time-step

2.3.F. Comparison of ANTARES results with literature examples

After having compared ANTARES results to the experimental ones, it was interesting to compare ANTARES results to similar studies that have been carried out by other research groups with other calculation tools. As SPERT III is practically the only experimental program with testing of rod ejections on a PWR core, it has already been widely used as a basis for experimental validation of calculation tools, which is great, because some validation studies very similar to this one with ANTARES, can be found in the literature, giving more comparison elements for ANTARES.

In particular, two articles have been chosen [41] and [42], because the study they present is a validation study similar to this one, and the test-case t60 was also used. As it can be seen on the graphs, ANTARES performances on the t60 test-case are similar to those achieved by other calculation tools. Interestingly, the deviation encountered with ANTARES is also similar to the one found in the literature. In fact, in both studies, it can be seen that the simulated power peak tends to be slightly delayed, and overshooting. Some more analysis will be carried out in the part 2.5, but it can already be concluded the performances of ANTARES in simulating the t60 test-case transient are quite encouraging for the following of the validation study.

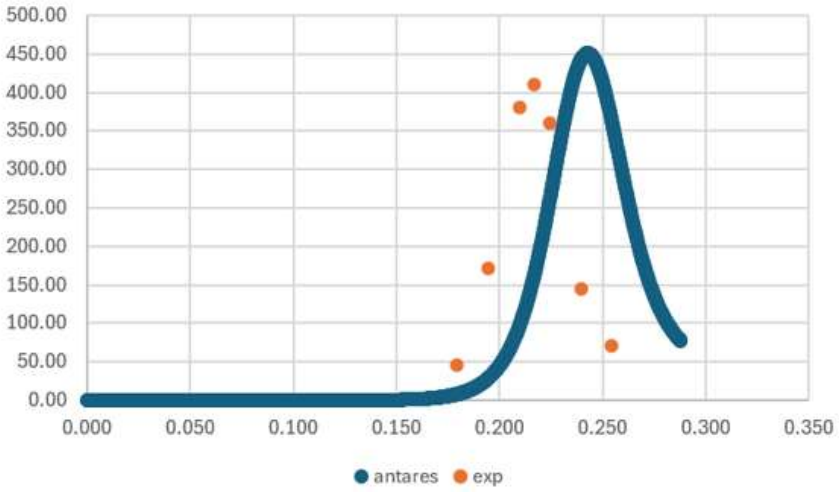

Figure 12. ANTARES-computed versus experimental power peak on the test-case t60

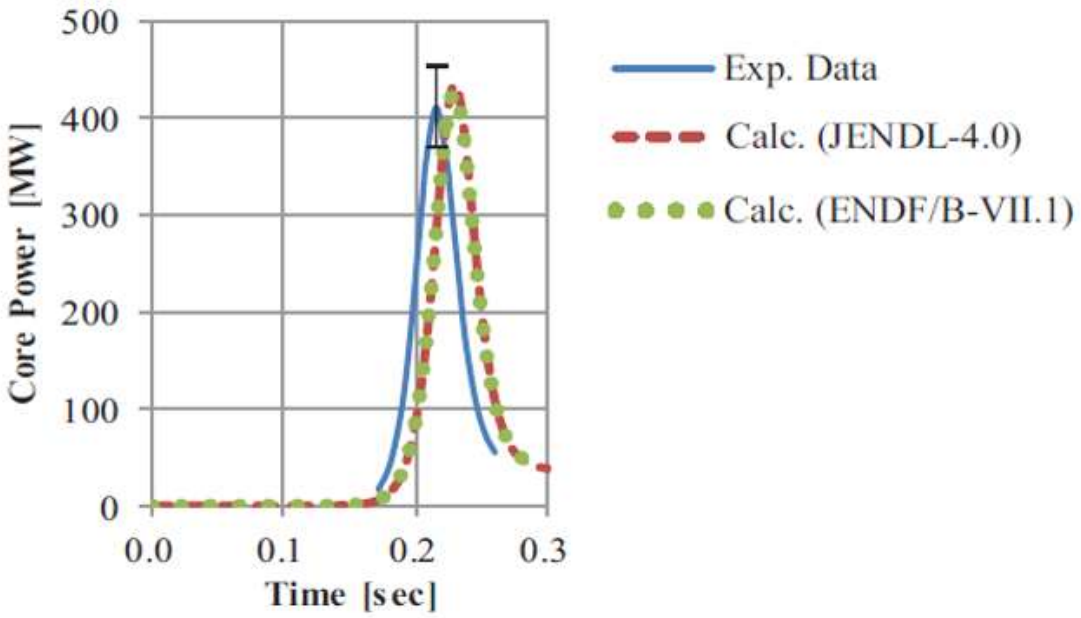

Figure 13. CASMO/TRACE/PARCS versus experimental results on case t60 [41]

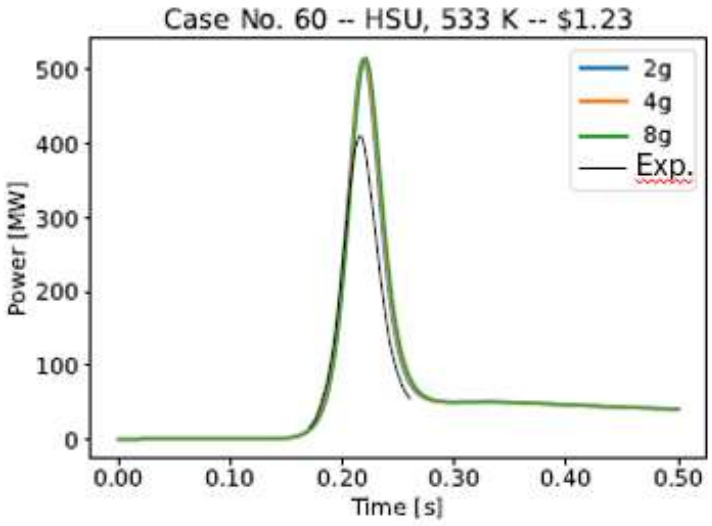

Figure 14. SIMULATE5X and CMS5 versus experimental results on case t60 [42]

2.4. Implementation of the other test-cases

The implementation process of the test-cases t70, t81 and t86 was similar to the one of t60. The main differences will be highlighted here. The 4 test-cases differ by their initial conditions, mainly the initial power and temperature, as can be seen in the table below.

	t60	t70	t81	t86
reactivity insertion ($)	**1.23** +/- 0.05	**1.21** +/- 0.05	**1.17** +/- 0.04	**1.17** +/- 0.04
temperature (°C)	**260** +/- 2	**120** +/- 2	**260** +/- 2	**260** +/- 2
power (MW)	**5,0E-05**	**5,0E-05**	**0.9** +/- 0.1	**19** +/- 1
power peak (MW)	**410** +/- 41	**280** +/- 42	**330** +/- 30	**601** +/- 60
power time (ms)	**227** +/- 5	**200** +/- 1	**135** +/- 3	**110** +/- 5

Figure 15. Main initial conditions and experimental results for the four selected test-cases

First, in order to know the mass flow rate of the water coolant, the density of the water has to be computed. For the test-cases t81 and t86, the temperature and pressure conditions are the same as for t60, giving the same density and mass flow rate. For the t70 test-case, the lower temperature gives a higher density of 948.45 kg/m3, and a proportionally higher mass flow rate, of 11.97 kg/s.

Then, the longest step was the determination of the rod clusters initial positions. The same method as for t60, described in the part 2.3.B, was used. The values found for z_ct (control rod cluster), and for z_tr (transient rod cluster, the one that is ejected during the test), are summed up in the next table. As a reminder, the positions are measured in extracted steps units, from 0 when the rod is entirely inserted to 101 when it is entirely extracted.

	t60	t70	t81	t86
z_ct	43.13	28.59	43.21	46.57
z_tr	32.9	24.87	33.56	36.14

Figure 16. Evaluated rod clusters initial positions for the four test-cases

From this point, it was possible to discretize the rod ejection, in a similar way as for t60, the ejection acceleration being the same constant of 50.8 m/s2. Having only a slightly different initial position, and the same acceleration, the ejection trajectory of the transient rod cluster, for each test-case, was very similar to the one found for the test-case t60 (cf part 2.3.C).

As for the simulation spatial mesh and time-step, the main configuration used was 80 axial meshes for PARCS, 30 for CATHARE, and a time-step of 0.1 ms. A slight improvement in the results was observed when increasing the number of axial meshes for CATHARE, in particular for

the test-cases t81 and t86, but the computations took much longer, for an improvement in the results that was not really significant. Thus, all the results presented here all use 30 axial mesh for CATHARE computations.

On the graphs of the Figures 18 to 21, are shown the comparisons between the obtained ANTARES results and experimental data, for each test-case, with the x-axis in ms and the y-axis in MW. It can be noted that there is only the peak point for the test-case t81, that is because the whole curve was not available in the experimental data. The times and heights of the power peak are summarized in the table of the Figure 17.

As it can be seen on the graphs below, ANTARES results on the test-cases t70, t81 and t86 are a bit less close to experimental results than those of t60. Not a lot of time was left to deeply inquire, but a higher initial power in the cases t81 and t86 could explain a more difficult ANTARES convergence. The computations for those two cases had to take more time for neutronics and thermo-hydraulics calculations to converge, and some tuning in the code parameters had to be modified to achieve a decent convergence. Some more tuning of the code parameters might be able to improve the results.

In spite of some deviations in the results, it can be said that the performance of ANTARES is not that bad, considering that the results could still be improved by a more in-depth setting of the code, and keeping in mind that this is a power peak simulation, which is a quite violent core transient. A very small variation in the initial parameters or the conditions of the test might cause large differences in the results obtained.

		t60	t70	t81	t86
	reactivity insertion ($)	**1.23** +/- 0.05	**1.21** +/- 0.05	**1.17** +/- 0.04	**1.17** +/- 0.04
	temperature (°C)	**260** +/- 2	**120** +/- 2	**260** +/- 2	**260** +/- 2
	power (MW)	**5,0E-05**	**5,0E-05**	**0.9** +/- 0.1	**19** +/- 1
(Exp.)	power peak (MW)	**410** +/- 41	**280** +/- 42	**330** +/- 30	**601** +/- 60
	power time (ms)	**227** +/- 5	**200** +/- 1	**135** +/- 3	**110** +/- 5
(ANTARES)	power peak (MW)	**450,8**	**376**	**271**	**445**
	power time (ms)	**242,7**	**285**	**169**	**127**

Figure 17. Main initial conditions and results for the four test-cases

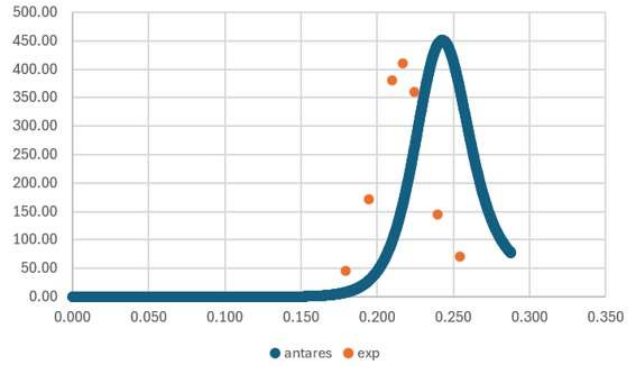

Figure 18. ANTARES versus experimental power peak, t60

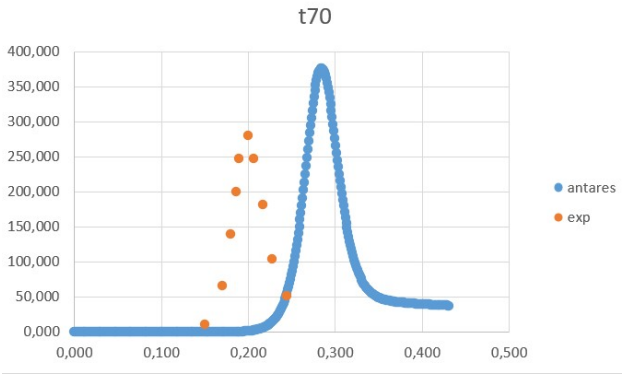

Figure 19. ANTARES versus experimental power peak, t70

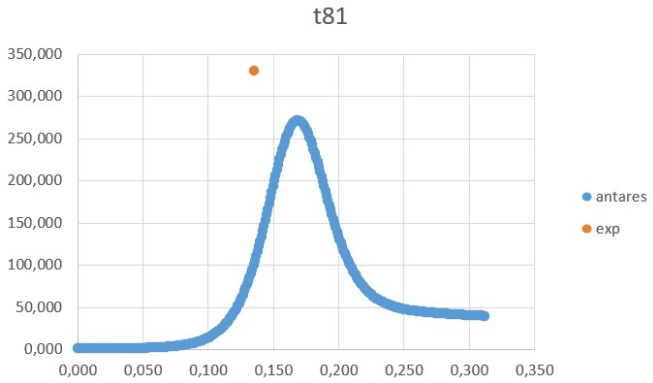

Figure 20. ANTARES versus experimental power peak, t81

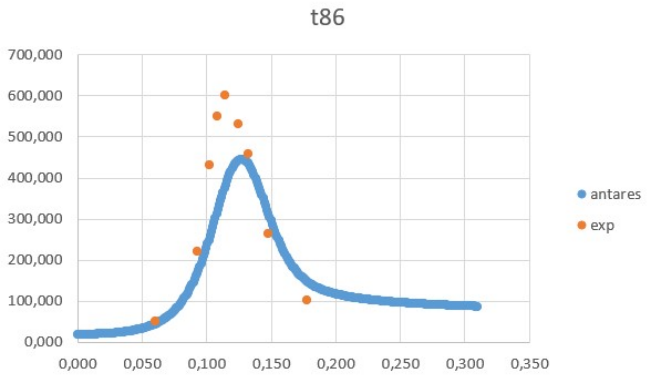

Figure 21. ANTARES versus experimental power peak, t86

2.5. Two small sensitivity analysis

In parallel with the testing of the test-cases t70, t81 and t86, as the first test-case t60 had already been studied, a couple small sensitivity analysis were conducted. In particular, the absence of uncertainty associated with the constant value of the rod ejection acceleration, as well as the fact that most of the simulated results seem to be late compared to the experimental ones, led to a sensitivity analysis on the acceleration value. Secondly, a small sensitivity analysis on the value of the inserted reactivity was carried out, in order to see how a small inserted reactivity variation would influence the results.

2.5.A. The rod ejection acceleration

As exposed in the part 2.3.C, the only experimental data given to describe the ejection of the transient rod cluster is the constant acceleration value, without any uncertainty. Moreover, it seemed that in all the test-cases, the simulated power peak was a bit late compared to the experimental one. The experimental value is 50.8 m/s2, used for all the test-cases. To see if a variation of this value could have a big influence on the results found by ANTARES, a test using an acceleration of 55 m/s2 instead of 50.8, was performed, all other parameters maintained unchanged. The ejection trajectory was regenerated, the ejection being now a bit faster (roughly 160 ms instead of 170).

As can be seen in the table below, the results obtained with the new value of the acceleration are very close to the base results. Even though the power peak is indeed happening slightly earlier with an acceleration of 55 m/s2, which is a big acceleration change, the variation in the results is too small to be significant.

acceleration (m/s2)	50,8	55
power peak value (MW)	450,8	458,6
power peak time (ms)	242,7	238

Figure 22. Change in ANTARES results with a variation in the value of the ejection acceleration

2.5.B. The reactivity inserted

During the experimentations with the code and the test-cases, it was interesting to see how large would be the change in the results if there was a difference in the reactivity inserted ; as this variable is probably one of the most influential on the results. Moreover, the experimental inserted reactivity is given with an uncertainty. For the t60 test-case, the inserted reactivity is 1.23 $, but with an uncertainty of 0.05 $, it could in reality be in the range 1.18$ to 1.28$ with a reasonable probability. Thus, the test-case t60 was simulated again, but with a modified value of the inserted reactivity, all other parameters maintained unchanged. A test with a 1.18$ inserted reactivity and one with a 1.28$ inserted reactivity were made. The process of determining the

initial positions of the rods had to be done in each case, as well as the discretization of the ejection trajectory. The initial positions of the rod clusters that were found are summarized in the table below.

inserted reactivity ($)	1,23	1,18	1,28
z_ct	43,129	42,995	43,248
z_tr	32,877	33,33	32,51

Figure 23. Change in initial rod positions with a variation in the value of the inserted reactivity

As it can be seen in the table of the Figure 24, a difference in the inserted reactivity results in a large variation of the simulated power peak value and time. In the experimental data, a power peak of 410 MW was observed 227 ms after the beginning of the transient rod cluster ejection. With ANTARES, if a 1,18$ inserted reactivity is used, the power peak is slower and smaller, and if a 1,28 $ inserted reactivity is used, the power peak is faster and higher ; and the deviations in the results are large. This is understandable, as the test-cases studied are violent transients, that are expected to be quite sensitive to initial conditions. In that context, the results obtained with ANTARES are quite satisfactory, for a preliminary study at least.

inserted reactivity ($)	1,23	1,18	1,28
power peak value (MW)	450,8	283,8	663
power peak time (ms)	242,7	277	218

Figure 24. Change in ANTARES results with a variation in the value of the inserted reactivity

General conclusion

The main goal of this internship was to contribute to the validation process of the multi-physics nuclear calculation tool ANTARES, with comparison to experimental test-cases from the SPERT III experimental program, on examples of rapid transient like a rod ejection. Considering that the internship happened at the very beginning of the experimental validation phase of ANTARES, the goal was also to setup some first calculations of SPERT III test-cases into ANTARES, in order to get some first results and understand the difficulties to tackle in the process.

In this context, some progress was made. After a preliminary "getting started with the tools" phase, a lot of tries and errors were made with the test-case t60 during the implementation phase, eventually leading to some first results, that were then refined with some further tuning of parameters. The results of this first ANTARES simulation of a SPERT III experimental transient were quite satisfactory, as the simulated power peak was rather close to the experimental one. The performance of ANTARES on this case was also similar to the one obtained in other studies existing in the literature, with other calculation tools.

In the final part of the internship, three more test-cases from the SPERT III experimental program were implemented into ANTARES, giving in the end more results. On these three test-cases, the simulated power peak was a bit less close to the experimental data, but still in a reasonable range. In parallel, two small sensitivity analysis were conducted, to better understand the sensibility of ANTARES results to the variation of certain parameters. A strong sensitivity was notably found with the value of the inserted reactivity during the rod ejection.

In the context of a preliminary experimental validation study of ANTARES, the internship brought some elements. In continuation, the results of the last three test-cases should be refined by checking deeply the tuning of the code, and more test-cases should be implemented, to increase the number of comparison elements in the scope of making progress in the global validation process of ANTARES.

From a more personal perspective, this internship was for me the occasion of working in nuclear research, which is a good addition to my Energy Engineering Master studies at Politecnico di Milano.

Bibliography

[1] The impact of the war in Ukraine on euro area energy markets

[2] Ampra Energy Renewable Energy vs. Fossil Fuels - Ampra EnergyRenewable Energy vs. Fossil Fuels - Ampra Energy

[3] Life Cycle Assessment of Renewable Energy Sources : (PDF) Life Cycle Assessment of Renewable Energy Sources

[4] Life Cycle Analysis of Wind Turbine : (PDF) Life Cycle Analysis of Wind Turbine

[5] Les différents types de pollutions et leurs impacts

[6] Whitepaper - Controlling the uncontrollable - BaxEnergy

[7] Is Nuclear Energy Renewable or Nonrenewable?

[8] How Does Nuclear Energy Affect the Economy? Exploring the Benefits and Challenges

[9] Going Nuclear? The long-term problem is political | Clingendael spectator

[10] List of software for nuclear engineering - Wikipedia

[11] F. Dubois, M. Forestier, G. Girault, J.C. Jaboulay, F. Jacq, A. Sargeni, "ANTARES: A New IRSN Computational Chain for Safety Analysis", *Proceedings of PHYSOR 2022*, American Nuclear Society, Pittsburgh, Pennsylvania, USA, *doi.org/10.13182/PHYSOR22-37270*

[12] Sûreté nucléaire — Wikipédia

[13] Loi n° 2006-686 du 13 juin 2006 relative à la transparence et à la sécurité en matière nucléaire (1). - Légifrance

[14] Loi 21 mai 2024 sûreté nucléaire, fusion ASN et IRSN | vie-publique.fr

[15] Autorité de sûreté nucléaire et de radioprotection - ASNR - ASN

[16] Accueil | IRSN

[17] Fission nucléaire — Wikipédia

[18] Nuclear cross section - Wikipedia

[19] Module 3 - Neutron Induced Reactions Rev 02.

[20] Fission Fragments and Products | Definition & Interactions | nuclear-power.com

[21] Neutron Cross Section - an overview | ScienceDirect Topics

[22] Nuclear Essentials - World Nuclear Association

[23] What is the difference between a thermal reactor and a fast neutron reactor?

[24] Pressurized water reactor - Wikipedia

[25] Sodium-cooled fast reactor - Wikipedia

[26] Six-Factor Formula - Effective Multiplication Factor | nuclear-power.com

[27] Prompt neutron - Wikipedia

[28] Delayed Neutrons | Definition & Characteristics | nuclear-power.com

[29] Delayed neutron - Wikipedia

[30] Effective Delayed Neutron Fraction – βeff - Beta Effective

[31] Dollar (reactivity) - Wikipedia

[32] On the development of multi-physics tools for nuclear reactor analysis based on OpenFOAM®: state of the art, lessons learned and perspectives - ScienceDirect

[33] Theory Manual - PARCS v3.0 U.S. NRC Core Neutronics Simulator.

[34] CASMO5 - Studsvik

[35] CATHARE (software) - Wikipedia

[36] 4826907

[37] osti.gov/servlets/purl/4570108/ *DUGONE, J. (Ed.), SPERT III Reactor Facility: E-Core Revision, AEC Research and Development Report IDO-17036, Phillips ; Petroleum Company, ID (1965)*

[38] Research Reactor Benchmarking Database: Facility Specification and Experimental Data (Revision) | IAEA

[39] guide 28 Guide de l'ASN n°28 - 03/09/2021 - ASN

[40] Laboratoire de Statistique et des Méthodes Avancées (LSMA) | IRSN

[41] Tatsuya Fujita & Tomohiro Sakai (2019) Analysis of the SPERT-III E-Core experiment using CASMO5/TRACE/PARCS based on JENDL-4.0 and ENDF/B-VII.1, Journal of Nuclear Science and Technology, 56:6, 553-571, DOI: 10.1080/00223131.2019.1598306

[42] (PDF) Initial Validation of SIMULATE5-K and the CMS5 Reactor Modeling Suite with the SPERT-III Experiments